

## Article

# Use of Spatio-Structural Parameters of the Multiscan Video Signal for Improving Accuracy of Control over Object Geometric Parameters

Vladimír Tlach <sup>1,\*</sup>, Michael Yurievich Alies <sup>2</sup>, Ivan Kuric <sup>1</sup>, Milan Sága <sup>3</sup>,  
Yuriy Konstantinovich Shelkovnikov <sup>2</sup>, Igor Olegovic Arkhipov <sup>4</sup>, Aleksandr Ivanovich Korshunov <sup>2</sup>  
and Anastasia Alekseevna Meteleva <sup>2</sup>

- <sup>1</sup> Department of Automation and Production Systems, Faculty of Mechanical Engineering, University of Žilina, 010 26 Žilina, Slovakia
- <sup>2</sup> Federal State Budgetary Institution of Science, Udmurt Federal Research Center of the Ural Branch of the Russian Academy of Sciences, Institute of Mechanics, Tatyany Baramzinoy 34, 426067 Izhevsk, Russia
- <sup>3</sup> Department of Applied Mechanics, Faculty of Mechanical Engineering, University of Žilina, 010 26 Žilina, Slovakia
- <sup>4</sup> Department of Software, Studencheskaya 7, Institute of Informatics and Computer Engineering, Kalashnikov Izhevsk State Technical University, 426069 Izhevsk, Russia
- \* Correspondence: vladimir.tlach@fstroj.uniza.sk

**Abstract:** In the present paper, we consider the issue of improving the accuracy of measurements and the peculiar features of the measurements of the geometric parameters of objects by optoelectronic systems, based on a television multiscan in the analogue mode in scanistor enabling. It is shown that the convolution of the input signal of the rectangular profile of the light zone with the impulse response of the multiscan explains the smearing of video signal edges. The value of smearing is completely determined by impulse response and does not depend on the zone width. It is established that signals of the action from narrow light zones are smeared out substantially relative to their width, and in this case, the conventional method for determining the zone width by the video signal derivatives stops working. A method is proposed for a full reconstruction of the rectangular profile of a light zone (including a narrow one) in a developed noise-proof optoelectronic measuring device based on a multiscan with the use of spatio-structural parameters, where the width of a light zone corresponds to an extent, illumination of the zone—to brightness, and its coordinate—to centroid. It is shown that the subtraction of the dissipation of the impulse response from the video signal dissipation allows for accounting of the value of the video signal smearing out with high accuracy at the estimation of the width of a light zone, in accordance with the property of the additive accumulation of dissipation. It is established that the use of the spatio-structural video signal model permits the extension of the application of multiscan-based optoelectronic devices for the high-accuracy control and measurement of the geometric parameters of small objects.

**Keywords:** multiscan; photodiode cell; light zone; video signal; impulse response; spatio-structural parameters



**Citation:** Tlach, V.; Alies, M.Y.; Kuric, I.; Sága, M.; Shelkovnikov, Y.K.; Arkhipov, I.O.; Korshunov, A.I.; Meteleva, A.A. Use of Spatio-Structural Parameters of the Multiscan Video Signal for Improving Accuracy of Control over Object Geometric Parameters. *Appl. Sci.* **2023**, *13*, 2994. <https://doi.org/10.3390/app13052994>

Academic Editors: Pavol Božek, Tibor Krenický and Yuri Nikitin

Received: 2 February 2023

Revised: 20 February 2023

Accepted: 23 February 2023

Published: 26 February 2023



**Copyright:** © 2023 by the authors. Licensee MDPI, Basel, Switzerland. This article is an open access article distributed under the terms and conditions of the Creative Commons Attribution (CC BY) license (<https://creativecommons.org/licenses/by/4.0/>).

## 1. Introduction

The development of devices for detecting the dimensions and shapes of industrial objects can be divided into two large groups: contact measurements and non-contact measurements. In the field of non-contact measurements, there are optical, laser, and camera systems. These systems have a wide range of applications [1–4] and are used for measurements of large objects or, conversely, of relatively very small ones. In our paper, we developed technical vision systems.

The development and introduction of high-speed technical vision systems for solving various problems in automation and integrated mechanisation of production processes and

robotics is a very important task [5–8]. Multi-scan (MS), a semiconductor analogue of a television camera tube, is designed to convert the illumination distribution on its photosensitive surface into an electrical video signal (VS) used for controlling, processing, and transmitting optical information in the technical vision systems, especially for contactless controlling and measuring of coordinates, dimensions, and movements of various objects [9–16]. Unlike charge-accumulating photoreceivers of the scanning type (charge-coupled devices and photodiode integral matrices), television scanistor structures such as solid scanistor and multielement MS are able to register an instantaneous illumination distribution in a wide range [12,14,17]. This permits the separation of amplitude-modulated optical signal information in intensive light noise conditions [12,18,19]. The wide use of noise-proof multiscan-based optoelectronic devices (MODs) in automated control systems is explained by the reliability of their operation, simplicity of the schemes of separating and processing measurement information, their compactness, and high metrological and performance characteristics [20–24]. In particular, laser MODs satisfy the industrial requirements for simplicity of operation and high metrological characteristics; in MODs, the spatial position of an object is reflected by the mirror surface of a passive reflection element (deflector) mounted on the object, and the laser MOD operation is based on the optical location principle. It should be noted that the determination of the object coordinates and dimensions in industrial conditions is a difficult challenge and of great importance [5,12,25,26]. It is shown in [12,15,17] that due to the limited steepness of the transition section of the multiscan photodiode cells, the I-V curve of the video signal from the rectangular profile of the light zone (LZ) is blurred and becomes bell-shaped. At the same time, the video signal from narrow light zones is blurred so significantly relative to their width, that the traditional method of determining the parameters of the LZ (coordinates, width, and illumination) from the derivatives of the VS ceases to work. The relevance of the problem becomes more acute in the case of measuring the geometric parameters of small objects in the condition of smeared image [27,28], for example: during contactless control over the diameters of fibres in the process of their manufacturing in fibre optics, the diameters of cables in the cable industry, the diameter of a narrow laser beam at its compression in laser optoelectronic systems in order to improve the signal/noise ratio, etc. To increase the accuracy when determining the width of blurred small-sized structural elements of various graphic images in [29,30], the possibility of using spatial-structural parameters (mass, centroid, dissipation, extent, and brightness) is considered. In [31], to solve the problem of the determination of the light zone dimensions and coordinates by the smeared-out video signal of the scanistor *p-n-p* structure, it was suggested using spatio-structural parameters (SSPs). The SSPs make it possible to estimate the width of the rectangular signal of an action, localize it in space and determine its amplitude by the smeared response of the path of the signal reception and transmission. The efficiency of using the SSPs is largely determined by taking into account the features of the multiscan operation in the time-pulse mode (in particular, the effect of changing the shape and amplitude of the VS when changing the width of the information LZ and the corresponding convergence of the transient functions of the multiscan). The purpose of the present paper is to improve the accuracy of measurements of the width, location, and brightness of LZ on the MS's photosensitive surface (corresponding to the geometric parameters of small objects) using the spatial and structural parameters of the video signal.

## 2. Features of the Multiscan Operation during the Determination of the Geometric Parameters of Objects

Television multiscan is an integrated circuit (Figure 1) containing two space-distributed solid resistive dividers of voltage,  $R1' - R(N + 1)'$  and  $R1'' - R(N + 1)''$ , and three lines of point *p-n* junctions,  $D1' - DN'$ ,  $D1'' - DN''$ , and  $D1''' - DN'''$ . To switch the signal current of each photodiode, two corresponding back-to-back switching diodes of the line,  $D1' - DN'$  and  $D1'' - DN''$ , are used; these are connected to the distributed resistive voltage dividers, and together with a photodiode compose a discrete cell. In an MS, a technique of scanning

the relief of light by the boundary of zero voltage [5,12,15] moving along the photosensitive surface by sawtooth voltage is used. To create the boundary, the parallel-connected MS resistive dividers are supplied with constant voltage  $E_0$  from the offset voltage source (OVS) to one of the pins, of which the sawtooth voltage generator (SVG) of polling with amplitude  $E_0$ , with the opposite polarity connected. The image of an object (Ob) illuminated by a radiation source (RS) is projected on the MS in the form of a light zone (LZ) with coordinates  $x_1, x_2$ , and of the edges of the controlled object. The switching of one more photodiode cell in the load circuit is performed by the zero voltage line at the moment when the saw-tooth voltage reaches the voltage level on the OVS cell. The cell photodiode switches from the closed to the open position, and the switching diodes from the open to the closed position.

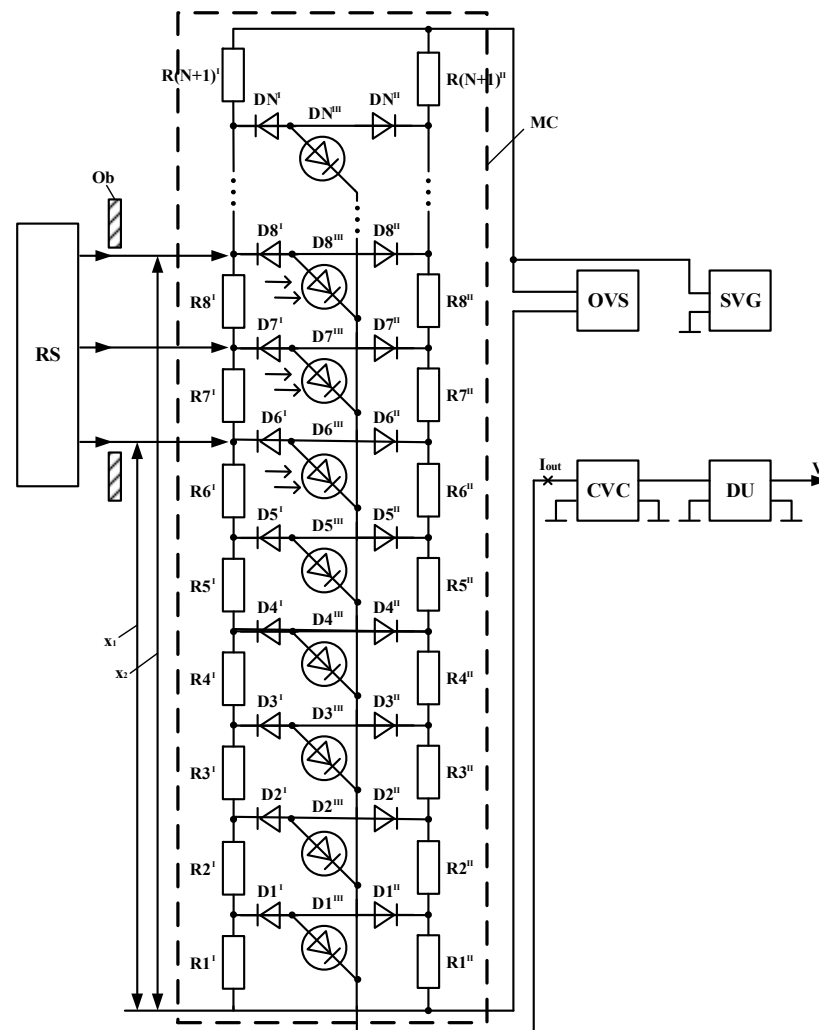


Figure 1. Enabling a multiscan using the “scanistor” scheme in the analogue mode.

Real MS is not an ideal device. There is a limited slope of switching of real I-V characteristics of photodiode cells, which determines the width of the volt-scanning aperture, equal to the quadruple temperature potential,  $E_0$  [12]. The formation of the MS output current  $I_{out}$  at the input of a current-to-voltage converter (CVC) is performed by the progressive switching of photodiodes by a sawtooth scanning voltage taking into account the volt aperture of photodiode cells. At the differentiation of the voltage from the CVC output by a differentiating unit (DU), due to the smearing of the transitional section of the I-V

characteristics of the cells, a bell-shaped video-signal (not rectangular) is formed reflecting the LZ profile uniform in brightness [5]:

$$V = \frac{4 \cdot L \cdot b \cdot l}{T} j_s \left[ \frac{1}{\exp[\alpha(E_e - E_c)] + 1} \right]_0^l + \frac{2 \cdot L \cdot b \cdot l_1}{T} (j_{bc}^f + j_{be}^f) \left[ \frac{1}{\exp[\alpha(E_e - E_c)] + 1} \right]_{x_1}^{x_2} \quad (1)$$

where  $L$  is the coefficient depending on the differentiation approach;  $b$  and  $l$  are MS width and length, respectively;  $l_1 = x_2 - x_1$  is the LZ width;  $\alpha = \frac{1}{U_0} = \left( A \frac{KT^\circ}{q} \right)^{-1}$ ;  $K$  is the Boltzmann constant;  $q$  is the electron charge;  $A$  is the coefficient reflecting the imperfection of the p-n junction of the scanistor structure;  $T^\circ$  is the temperature in Kelvin;  $E_e = E_0 \cdot \frac{x_0}{T}$  is the emitter potential at the polling point  $x_0$ ;  $E_0$  is the constant bias voltage of the emitter;  $E_c = E_0 \cdot \frac{t_0}{T}$  is the sawtooth voltage value at polling moment  $t_0$ ;  $T$  is the sawtooth voltage period;  $j_s$  is the density of dark saturation current of photodiode cell;  $j_{bc}^f$  and  $j_{be}^f$  are the increment density of saturation currents of the base-collector and base-emitter junctions, respectively, at illumination; and  $x_1$  and  $x_2$  are the coordinates of LZ beginning and ending on the MS, respectively. The duration of the time interval from the initial sawtooth voltage to the VS maximum is proportional to the distance between the LZ middle and the MS beginning.

Due to its dual character, the MS discrete-solid structure has a discrete or analogue shape of a VS depending on the step voltage between photodiode cells. In [5] it is shown that when the step voltage decreases to the value of  $\frac{E_0}{N} < 4U_0$  (where  $E_0$ —bias voltage of resistive divider;  $N$ —number of structure cells;  $4U_0$ —voltage at the transitional section of I-V characteristics of the cell), the discreteness of the MS structure is not manifested and its output current has an analogue character. In the analogue mode, bell-shaped VSs from neighbouring switching discrete cell overlap each other and the total VS becomes trapezoidal. The condition of the analogue mode is a potential distribution on a solid divider, and any time that the sawtooth voltage is polling, there are no less than two cells in the current-switching state. The first feature of the MS in the analogue mode is high coordinate-dimension sensitivity to the movements of LZs corresponding to the geometric parameters of controlled objects. The analogue mode provides a high accuracy in the measurement of these geometric parameters, namely, coordinates, dimensions, movements, and simultaneously the energy parameters of one or more LZs. The second feature of the MS connected with the analogue mode, is the noise-proofing of MS-based measuring devices in contrast to other photoreceivers of the scanning type, such as charge-coupled devices (CCD) and photodiode matrices (PDM) based on the principle of charge accumulation, which do not allow for registering information from fast-changing light fields. An MS can operate in a wide dynamic range (more than 80 dB) of the intensities of light signals at the frequency range of the intensity variation of more than 100 kHz [12]. MS-based optoelectronic devices provide the specified accuracy in obtaining measurement information in the conditions of strong light noises by brightness modulation of light radiation and subsequent synchronous detection. The third feature of MS in the analogue mode is the change of the VS shape (from a trapezoidal to a bell shape) at the decrease of the width of the uniform-in-brightness LZ (from maximal, which corresponds to the fully illuminated MS, to minimal, when the zone is absent).

Analysing the formation of the VS trapezoidal and bell shapes, it is practical to replace the second member in Formula (1) with the difference of the MS transition functions ABC and CDE (Figure 2), which can be represented as the responses to the input action in the form of two contrasts, light and shade of the MS light zone in the coordinates  $x_1$  and  $x_2$ . The results of modelling in Mathcad the effect of the change of the VS shape and amplitude at the change of the LZ width, and the corresponding convergence of the transition functions show the following: At the LZ width exceeding the volt aperture (VA)  $VA \geq 8U_0$ , a video signal has a trapezoidal shape. At the contact of the transition functions, the VS acquires a bell shape. At a further decrease in the LZ width to the moment of its disappearance, the

VS bell shape is retained, but its width and amplitude are decreasing non-linearly with the decrease in LZ width. In the literature on television scanistor structures, this dimensional region of light zones (when the video signal is bell-shaped) is commonly referred to as the region of narrow LZ (the region of small objects) in contrast to the region of wide zones with trapezoidal VSs.

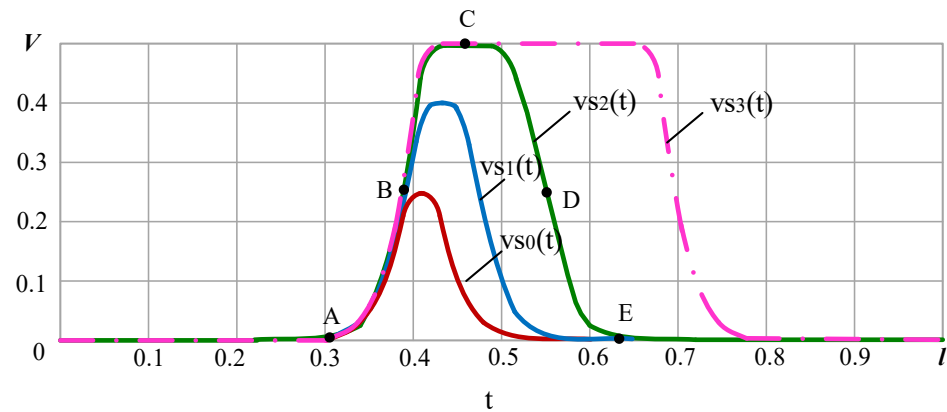


**Figure 2.** The change of the shape and amplitude of a video signal with the change of the light zone width.

Narrow LZs are widely used for high-accuracy noise-proof measurements of the coordinates of objects because of the high sensitivity of the MS to the movements of such zones. It is also possible with the use of an optical system, by decreasing the LZ width, to increase the zone brightness and the signal/noise ratio (especially by using an LZ in the form of narrow laser lines); in this case, at the zone brightness variation, the maximum of the bell-shaped VS always corresponds to the zoned middle in brightness. However, a considerable drawback of measuring the geometric parameters of small objects is the non-linearity of the dependence of the VS width and amplitude on the LZ width change, and the corresponding insufficient accuracy of the measurements. The problem of determining the width and brightness for narrow LZs with a high accuracy requires further investigation, and is currently of importance (particularly for measuring the diameters of items in fibre-optics and the cable industry, as well as in refractometers—colorimeters for finding the coordinates and brightness of the information beam, etc.). It should be also noted that for improving noise-proofing and accuracy of industrial measurements of the geometric parameters of small objects in the conditions of strong noise, the use of brightness modulation of light radiation is practical [18,19].

### 3. Results and Discussion

The structure diagram of the developed noise-proof optoelectronic device based on MS (MOD) for measuring the geometric parameters of objects is shown in Figure 3 (where Ob—controlled object; MS—multiscan; BMLS—brightness-modulated light source; BVS—bias voltage source; SVG—sawtooth voltage generator; GMP—generator of modulating pulses; CVC—current-voltage converter; BPF—bandpass filter; SD—synchronous detector; LPF—low-pass filter; ADC—analogue-to-digital converter; MP—microprocessor). The MS-based optoelectronic device MOD operates as follows: A parallel beam from the brightness-modulated light source BMLS forms a light zone LZ on the photosensitive multiscan MS surface. The beginning  $x_1$  and the end  $x_2$  of the zone correspond to the geometric parameters of an object Ob. An intensity-modulated information component of the collector current, separated at the polling of the multiscan MS, is converted into voltage in the current-voltage converter CVC. After filtration by the band-pass filter BPF and demodulation using the synchronous detector SD, the voltage enters the analogue-to-digital converter ADC input and then the microprocessor MP for processing the measurement information. The use of light flux modulation allows for decreasing errors in the measurement of the LZ parameters,

which arise due to the dark current non-uniformity of the MS photodiode cells at weak light fluxes, and also in the case of light noise. The MOD drawback is a decrease in the accuracy of measurements of the parameters of small objects.

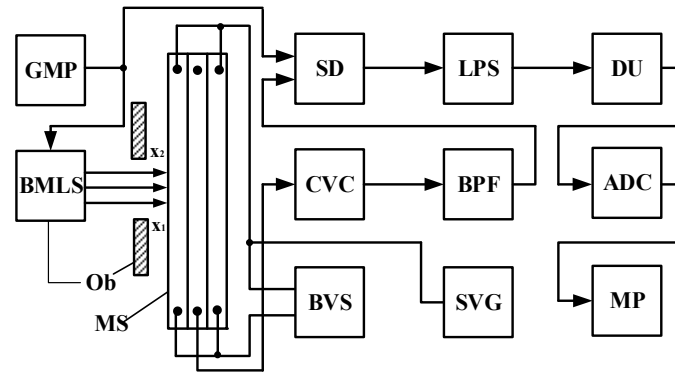


**Figure 3.** Structure diagram of the noise-proof multiscan-based device for measuring the geometric parameters of objects.

To provide high-accuracy measurements by the MOD, the linearity of the spatio-temporal conversion of the measurement information about an object *Ob* is the most important; such a conversion consists of two stages of the photoelectric conversion of the measured dimension (or coordinate) of the object within a time interval. In the first stage, the coordinate of the controlled light zone on the multiscan is converted to the linear coordinate-specifying voltage on the solid resistive dividers  $R' - R(N + 1)'$  and  $R'' - R(N + 1)''$  (Figure 1), which provide the MS high sensitivity to the zone movements. The second conversion of the above voltage is performed by a scanning sawtooth polling voltage from the SVG with the use of the volt aperture within a time interval. The general error in the conversion of the LZ coordinate  $x$  within the time interval  $t_x$  is determined by the linearity of the coordinate characteristics CC:

$$x = t_x \cdot l / T \tag{2}$$

At the idealized I-V characteristics of photodiode cells (described by a Heaviside function), a VS from them would have the form of a Dirac delta function; however, due to the limited slope of the transitional section of the I-V characteristics of the cells, the VS is smeared out and acquires a bell shape. The value of the VS smearing-out due to the influence of the volt aperture (at the contact of transition functions) is  $8U_0$  and is described by the MS aperture response AR. It should be noted that the most important electrophysical characteristics of the MS are coordinate characteristics CC and aperture response AR. The CC reflects the linearity of the photoelectric transformation of the coordinates of the object image within the VS time intervals at the time-pulse mode of the MS operation. The AR determines the MS ability to reproduce small details of the image. From this point of view, the MS can be characterized by unit resolution, number of resolved lines, and aperture width.

At first, television scanistor structures (TSSs) were developed only for televisions [12,14] as solid-state analogues of television camera tubes, and their main characteristic was aperture response (i.e., the dependence of the depth of the VS modulation on the spatial frequency of the line target). As for all television camera tubes, the main TSS parameter was television resolution capability (determined with the use of the linear line target by the number of lines per 1 mm at twenty percent VS modulation). AR is determined by the shape and finite sizes of a scanning element, i.e., by its aperture. In the MS the scanning element is the scanning boundary or the line of zero potential. In the TSS there are volt  $U_0$  and linear  $b$  apertures:

$$U_0 = 4KT / q \tag{3}$$

$$b = U_0 \cdot l / E_0 \tag{4}$$

Equation (3) is a volt expression of the aperture of the scanning boundary determined by the value of the smearing of the I-V characteristics of the MS photodiode cell equal to the quadruple temperature potential. The linear aperture (expression (4)) is the minimum size of the projection of a measured object, at which the VS edges are not distorted yet, and consequently, the correspondence between the size of the object projection and the video pulse duration is retained.

The analysis of the modelling results has shown that a VS is actually a smeared profile of the LZ, and the task of its analysis is to determine the zone parameters (coordinates, width, and illumination) by the smeared-out bell-shaped VS from the MS. Figure 4c,d illustrate the stages of the conventional processing of the VS with the use of its first and second derivatives. It can be seen that the width of the wide LZ can be determined using the difference of the moments of the time of zero crossings of the trapezoidal VS second derivative; it can also be determined directly by the VS (without its differentiation) if the measured moments of time correspond to the VS crossing half its maximum. In this case, for the wide LZ, the VS amplitudes and first and second derivatives are directly proportional to illumination. However, for narrow zones, the moments when the sign of the second derivative of the bell-shaped VS change do not correspond to the boundaries of these zones since the TSS cannot register their width with a high accuracy, due to the VS smearing out by its volt aperture. The time coordinate of the middle of the narrow LZ is definitely determined by the moment of the VS first-derivative zero crossing.

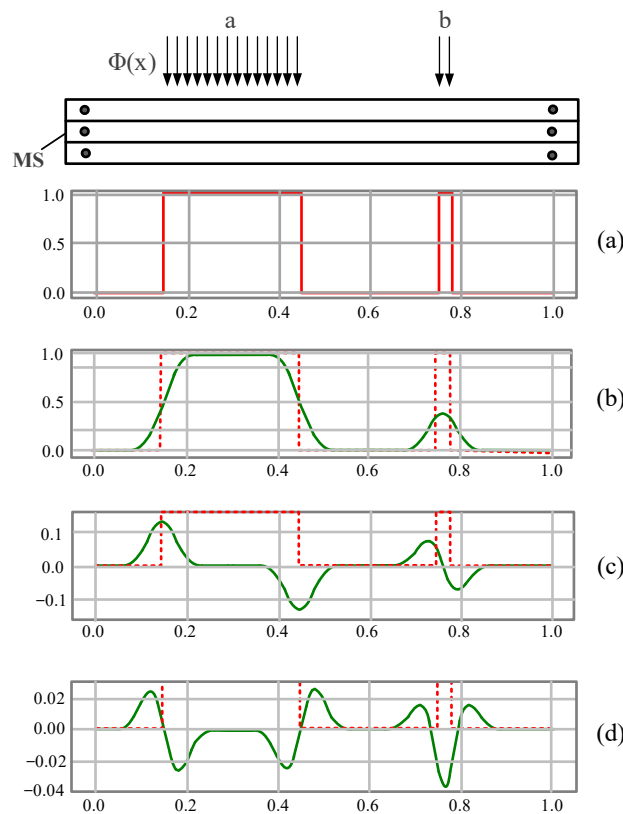


**Figure 4.** Timing diagrams illustrating the operation of a noise-proof multiscan-based measuring device. (a) the action  $f(x)$  is the profile of the light zone; (b) the response  $V(t)$  is the MOD video signal (solid line); (c,d) illustrate the stages of the conventional processing of the video signal with the use of its first and second derivatives.

Thus, the conventional processing of the VS of small objects does not permit the provision of a high potential accuracy of the MOD; therefore, it is practical to study the mechanism of

the formation of a smeared-out VS for improving the metrological characteristics of measuring devices.

3.1. The Mechanism of the Formation of the Multiscan Video Signal on the Basis of Its Impulse Response

One of the most important problems of MODs is their reduction to an ideal device, i.e., the exclusion of the influence of the device circuit from the measurement results. The reconstruction of the real LZ relief using its convolution with impulse response (IR) (i.e., using a VS) is called ‘deconvolution’. For such reconstruction, it is necessary to know the parameters of the IR. The problem of deconvolution can be solved by the transformation of the convolution integral [31]:

$$v(t) = \int_0^{\infty} f(x)h(t - x)dx \tag{5}$$

where  $f(x)$  is the initial distribution of the LZ illumination which should be reconstructed;  $h(t - x)$  is the IR that specifies distortions;  $v(t)$  is a VS from the MS.

The primary task of the reconstruction of the LZ geometric parameters is the determination of its coordinates in the process of scanning. The MOD is a linear system with constant parameters, and it can be represented in the form of a structural diagram (Figure 5a).

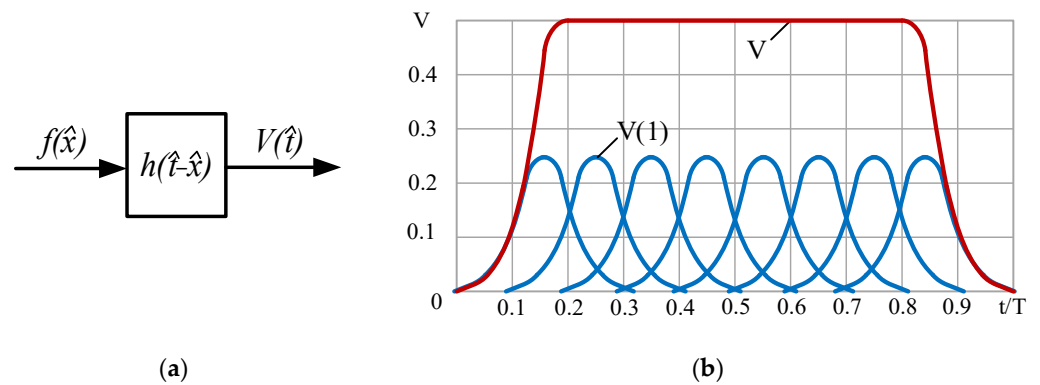


Figure 5. The mechanism of the multiscan video-signal formation: (a) the scheme of the convolution of the impulse response and light zone parameters; (b) the sum video signal V of the multiscan and the elementary video signals V(1) of its photodiode cells.

In this case, the action  $f(\hat{x})$  is the profile of the LZ (dashed line in Figure 4b), the response  $V(\hat{t})$  is the MOD video signal (solid line), and the MOD work is described by the IR  $h(\hat{t} - \hat{x})$  (where  $\hat{x} = \frac{x_0}{T}$  is the normalized coordinate of the polling point  $x_0$ , and  $\hat{t} = \frac{t_0}{T}$  is the normalized time of polling  $t_0$ ). The MOD impulse response is the function  $h(\hat{t} - \hat{x})$ , which is the system response to an input signal in the form of a unit Dirac delta pulse. For the MOD, such a pulse is an output signal  $V_C$  from an infinitely narrow LZ (i.e., a VS from one MS photodiode unit cell). In this case, the VS at the MOD output can be represented in the form of the convolution of an input signal (the light relief on the photosensitive MOD surface) and the system impulse response.

To determine the multiscan IR, we wrote the system of equations of currents and voltages for its photodiode unit cell in a scanistor enabling (Figure 6).

$$E_c = E_{e0} + U_{be} + U_{bc} \tag{6}$$

$$j_{be} = j_s (e^{\alpha U_{be}} - 1) - j_{be}^f \tag{7}$$

$$j_{bc} = -j_s (e^{\alpha U_{bc}} - 1) + j_{bc}^f \tag{8}$$

$$j_{out} = 2j_{bc} \tag{9}$$

where  $E_{e0} = E_0 \frac{x_0}{T}$  is the potential of the dividing layers  $R'_i$  and  $R''_i$  at the polling point  $x_0$ ;  $E_c = E_0 \frac{t_0}{T}$ —the value of the sawtooth voltage at the moment of polling  $t_0$ ;  $T$ —period of sawtooth voltage;  $j_{be}$  and  $j_{bc}$ —total currents through base-emitter and base-collector junctions, respectively;  $U_{be} = U_{be1} = U_{be2}$ —base-emitter junction voltage 1, 2;  $U_{bc}$ —base-collector junction voltage;  $j_s = j_{be}^s = j_{bc}^s$ —dark saturation current density of base-emitter and base-collector junctions.

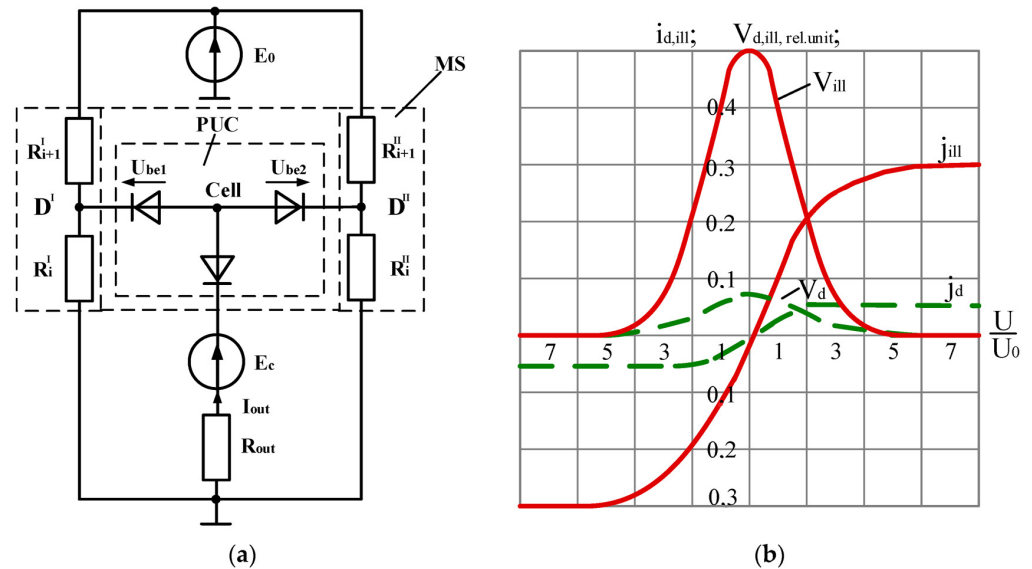


**Figure 6.** Equivalent scheme of the multiscan photodiode unit cell in scanistor enabling: (a) full scheme; (b) volt-ampere characteristics and video signal (in darkness—dashed line; at illumination—solid line).

From Equations (7) and (8) we obtain the following:

$$U_{be} = \frac{1}{\alpha} \ln \frac{j_{be} + j_{be}^s + j_{be}^f}{j_{be}^s} \tag{10}$$

$$U_{bc} = \frac{1}{\alpha} \ln \frac{j_{bc}^s - j_{bc}^f - j_{bc}}{j_{bc}^s} \tag{11}$$

By substituting Equations (10) and (11) into (6) and solving the latter with respect to  $j_{bc}$ , we obtain an expression for the output current  $j_{out}$  and the video signal  $V_s$  of the unit cell:

$$j_{out} = 2 \left( j_s \frac{\exp \alpha(E_c - E_e) - 1}{\exp \alpha(E_c - E_e) + 1} + j_{bc}^f \frac{\exp \alpha(E_c - E_e)}{\exp \alpha(E_c - E_e) + 1} - j_{be}^f \frac{1}{\exp \alpha(E_c - E_e) + 1} \right) \tag{12}$$

$$V_{cell} = L \frac{dj_{out}}{dt} = L \frac{2E_0}{U_0 T} \cdot \frac{\exp \alpha(E_c - E_e)}{[\exp \alpha(E_c - E_e) + 1]^2} \cdot [b(2j_s + j_{be}^f + j_{bc}^f)] \tag{13}$$

where  $L$  is the coefficient depending on a differentiation approach (in the ideal case,  $L = 1$ ).

A video signal from one MS photodiode unit cell has two limiting cases. In the first case, when IR does not cause distortions (i.e.,  $h(\hat{t} - \hat{x}) = \delta(x)$ , where  $\delta(x)$  is the unit Dirac delta function), an ideal measurement by the MOD takes place. Equation (13) for a VS from one cell is then transformed into real rectangular light relief from a uniform LZ:

$$V_{cell} = j_{cell}(x) = b(2j_s + j_{be}^f + j_{bc}^f) \tag{14}$$

In the second case, when the measured input quantity is in the form of the Dirac delta function (i.e.,  $j_f(x) = \delta(x)$ ), Equation (13) is transformed into the multiscan impulse response:

$$V_{cell} = L \frac{dI_{out}}{dt} = \frac{2E_0}{U_0 T} \cdot \frac{\exp \alpha(E_c - E_e)}{[\exp \alpha(E_c - E_e) + 1]^2} \tag{15}$$

The VS of the string television MS is the LZ convolution with IR:

$$\begin{aligned} V(\hat{t}) &= L \int_0^l j(\hat{x}) \cdot h(\hat{t} - \hat{x}) dx = L \left[ b \left( 2j_s + j_{be}^f + j_{bc}^f \right) \right] \cdot \frac{2E_0}{U_0 T} \int_0^l \frac{\exp \alpha(E_c - E_e) dx}{[\exp \alpha(E_c - E_e) + 1]^2} = \\ &= 2Lbj_s \left[ \frac{2Ll}{T} \cdot \frac{1}{\exp \alpha(E_c - E_e) + 1} \right]_0^l + b \left( j_{be}^f + j_{bc}^f \right) \left[ \frac{2Ll_1}{T} \cdot \frac{1}{\exp \alpha(E_c - E_e) + 1} \right]_{x_1}^{x_2} \end{aligned} \tag{16}$$

It can be seen that Equation (16) coincides with (1) for the multiscan VS and shows the correctness of the obtained expressions for IR and LZ. Figure 5b shows the process of the formation of a trapezoidal video signal as the sum (integral) of IRs, i.e., video signals from photodiode unit cells.

The convolution of the signal of the LZ profile with impulse response explains the smearing of the edges of the MOD video pulse. The quantity of the smearing is fully determined by the MOD IR and does not depend on the LZ width. Thus, the smearing-out of the signals of the action of narrow light zones relative to their width is so significant that the conventional method for the determination of the LZ width by the first and second derivatives of the MOD video signal stops working (see Figure 4c,d).

### 3.2. Results of the Use of Spatio-Structural Parameters of the Multiscale Video Signal for Improving the Accuracy of the Measurements of the Geometric Parameters of Objects

The developed MOD (Figure 3) is a linear system with constant parameters, which can be represented in the form of a structural scheme (Figure 5a). In this case, the MOD work is described by the impulse response  $h(\hat{t} - \hat{x})$ , the action  $f(\hat{x})$  is the light zone profile (dashed lines on the diagrams in Figure 4b and the response  $v(\hat{t})$  is a MOD video signal (solid line).

In [31], to solve the problem of the determination of the light zone dimensions and coordinates by the smeared-out video signal of the scanistor *p-n-p* structure, it was suggested to use spatio-structural parameters (SSPs). The SSPs make it possible to estimate the width of the rectangular signal of an action, localize it in space and determine its amplitude by the smeared response of the path of the signal reception and transmission. The SSPs are functionals, the values of which depend on the parameters of the transformation of measurement signals acting in reception and transmission systems. Such transformations are the weighing and summing of signals, the transformation of bias and scaling of signals, and convolutions of signals with the impulse responses of the linear units of the system of signal reception and transmission. The SSPs are integral characteristics of signals and are constructed based on the moments of a different order [29,30]. The moments are described by the following expressions:

$$W_k = \int t^k f(t) dt \tag{17}$$

where integration is performed over the entire interval of the signal observation (finite or infinite; in the first case,  $f(t)$  is assumed to be equal to zero beyond the interval).

In [31], five SSPs of a video signal are determined: mass ( $M$ ), centroid ( $C$ ), dissipation ( $D$ ), extent ( $E$ ) and brightness ( $Y$ ). The SSPs are computed using one-dimensional moments  $W_0$ ,  $W_1$ , and  $W_2$  by the following expressions:

$$M = W_0 \tag{18}$$

$$C = W_1 / M = W_1 / W_0 \tag{19}$$

$$D = W_2 / M - C^2 = W_2 / W_0 - (W_1 / W_0)^2 \tag{20}$$

$$E = 2\sqrt{3D} = 2\sqrt{3(W_2/W_0 - (W_1/W_0)^2)} \tag{21}$$

$$Y = \frac{M}{E} = \frac{W_0}{2\sqrt{3(W_2/W_0 - (W_1/W_0)^2)}} \tag{22}$$

In the above expressions, the second variant is only a function of the moments, and the first variant is a recurrent scheme of computations, in which each subsequent parameter is expressed in terms of the former ones. The SSPs' interpretation is as follows:

- the signal mass is an integral over the entire signal observation interval (in this case, it is necessary to take into account that the mass function is unipolar); the physical analogue of the signal mass is the total mass of a linear object with a certain specified mass distribution over its length, which is described by the density of its redistribution  $f(t)$ ;
- the signal centroid corresponds to the "centre of gravity" of the indicated linear object;
- the signal dissipation characterizes the degree of the dispersion of the masses around the "centre of gravity" of the indicated linear object; the smaller the dissipation value is, the larger the part of masses around the "centre of gravity" is localized; and vice versa, the larger the dissipation value is, the more dispersal character of the mass distribution is.

When mass, centroid, and dissipation are suitable for the description of signals with a random distribution of amplitudes over their entire length, it makes sense to compute the extent and brightness for rectangular signals which are light zone profiles on the multiscan (Figure 4a). In the case of specified limitations for the measurement signal shape, the extent corresponds to the width of the rectangular signal (light zone width) and brightness to its amplitude (light zone illumination).

Of all the SSPs, the most interesting is dissipation due to its property to take into account the value of the smearing-out of a video pulse when it passes through the path of reception and transmission in the MOD with the impulse response  $h(\hat{t} - \hat{x})$  (Figure 5). In this case, the output signal dissipation  $v(\hat{t})$  is:

$$D[v(\hat{t})] = D[f(\hat{x})] + D[h(\hat{t} - \hat{x})] \tag{23}$$

Let us summarize the case described in Figure 5 and expression (23) when the video pulse  $f(\hat{x})$  passes through the sequence of linear units with the impulse responses  $h(\hat{t} - \hat{x}_i)$  (Figure 7).



Figure 7. Generalized model of the multiscan-based optoelectronic device.

In this case, the dissipation of the system response is described by the following expression:

$$D[v(\hat{t})] = D[f(\hat{x})] + \sum_{i=1}^n D[h(\hat{t} - \hat{x})] \tag{24}$$

Expression (24) demonstrates the main dissipation property—the property of additive accumulation when the signal is passing through the sequence of linear units. Thus, observing the smeared-out signal registered by the MOD, and knowing the impulse response of the MOD, it is possible to compute the real values of light zone width and brightness.

The dissipation property of additive accumulation is very important for the estimation of the video pulse parameters  $f(\hat{t})$  by the observed MOD response  $v(\hat{t})$ . In [31] it is shown that SSPs allow a sufficiently accurate estimation of the duration of narrow rectangular pulses by their smeared-out video pulses. Using the spatio-structural MOD model, it is assumed

to describe the MOD video signal in the form of the SSP vector  $S_v = (M_v, C_v, D_v, E_v, Y_v)$ , and the MOD pulse response in the form of the vector  $S_h = (M_h, C_h, D_h, E_h, Y_h)$ . The SSP vector of the observed MOD response  $S_v$  is computed by the MOD video signal, and vector  $S_h$  by the MOD pulse response (1, 15). In this case, it is possible to estimate the light zone width and illumination as follows:

- LZ profile “dissipation”:

$$D_f = D_v - D_h \tag{25}$$

- LZ profile “extent”:

$$E_f = 2\sqrt{3D_f} \tag{26}$$

- LZ profile “brightness”:

$$Y_f = \frac{M_v}{E_f} \tag{27}$$

- LZ profile “centroid”:

$$C_f = C_v \tag{28}$$

In Equation (25) the operation of the subtraction of the pulse response dissipation  $D_h$  from the video signal dissipation  $D_v$  allows us to take into account the value of the VS smearing-out by the reception system when the light zone width is estimated in accordance with the property of additive accumulation of dissipation.

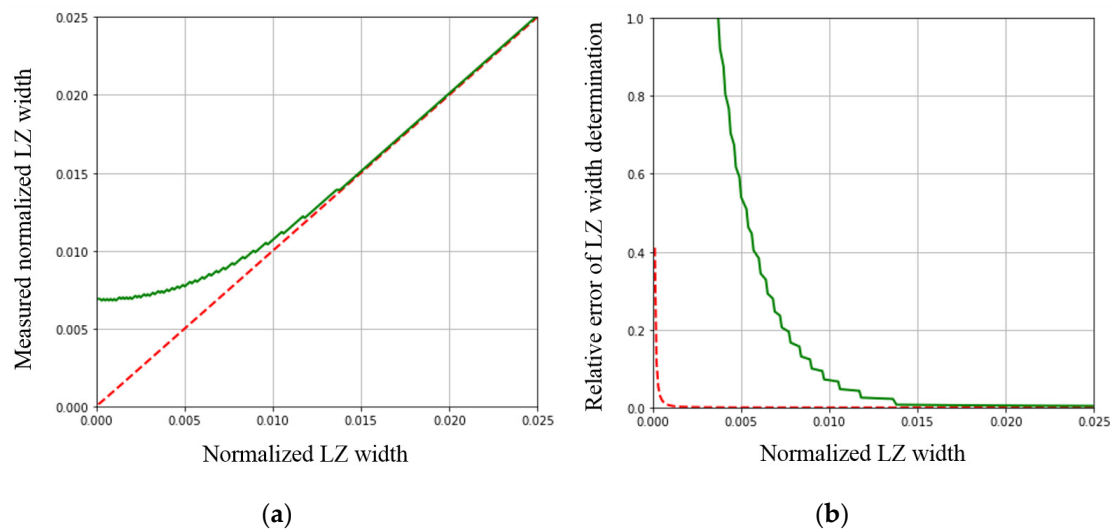
The light zone coordinate and width of the multiscan are traditionally determined by the first or second derivatives of the MOD video signal OUM  $v(\hat{t})$  (Figure 4c). However, in [31] it is also shown that the narrow light zone width determined by the VS derivatives is significantly overestimated. Moreover (as it follows from Figure 2), in the case of a narrow LZ, the amplitude of the observed MOD response  $v(\hat{t})$  significantly decreases and its reconstruction directly by the signal  $v(\hat{t})$  is impossible. Nevertheless, the first and second derivatives of the video signal  $v(\hat{t})$  allow a highly accurate determination of the coordinates of the middle of the zone (including a narrow zone), which is widely used in equipment.

In the present paper, a method is offered for a full reconstruction of the light zone profile (both wide and narrow) with the use of SSPs. The width of the zone profile corresponds to the extent, and is determined by expressions (25) and (26); brightness by Formula (27), and the coordinate of the middle by expression (28).

A number of experiments were carried out for the reconstruction of the LZ profile geometry and spatial location on the multiscan. With this purpose, on the MS photosensitive surface, a light zone was formed which was gradually broadening. The multiscan width was taken as 1 and the measurements of the zone coordinates and width were performed in the relative units of its length. The light zone width varied from 0.00001 to 0.1 depending on the multiscan length, and its video signal was digitized and processed by the digital method with the use of the MP (Figure 3). For the reconstruction of the light zone profile and the coordinates of its middle, both the conventional approach with the use of the first derivative of the VS and the alternative method with the use of the SSPs offered in the present paper were used.

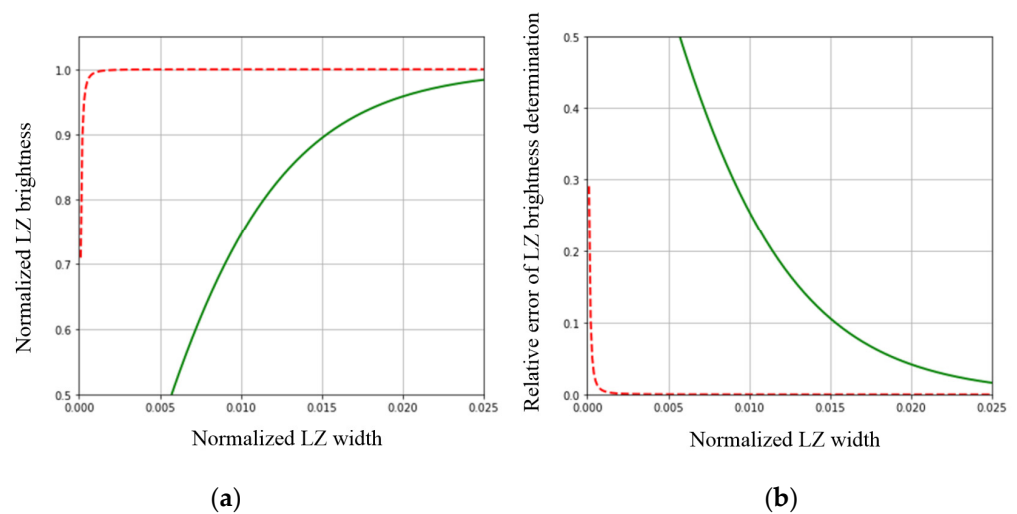
Figure 8 shows the measurement results for the normalized value of the LZ width, which has been measured in accordance with expressions (25) and (26) for the SSPs. In the case of the conventional method for measuring the light zone width, the observed multiscan video signal  $v(\hat{t})$  was differentiated; after that, the extrema of the first derivative of the video signal were determined. The extrema coordinates were taken as the light zone boundaries. From the analysis of the diagrams in Figure 8a it follows that the reconstruction of the LZ width using the SSPs (dashed line) is in accordance with the law close to the linear law

over the entire range of the zone width values (in the region of narrow zones as well). At the same time, it can be seen that in the conventional method for the reconstruction of a light zone width (solid line on the diagrams in Figure 8a), the zone width is characterized by non-linear dependence, which gives a significant overestimation of the width value for narrow zones. The diagrams of the relative error at the light zone reconstruction are given in Figure 8b and indicate the high accuracy of the zone width reconstruction with the use of the SSPs, even in the region of very narrow LZs. It should also be noted that in the region of wide LZs, both methods provide the possibility of estimating the zone width with a high accuracy and sufficiently close to the real values. Therefore, in the diagrams in Figure 8, the range of the normalized values of the LZ width is limited by the value 0.025.



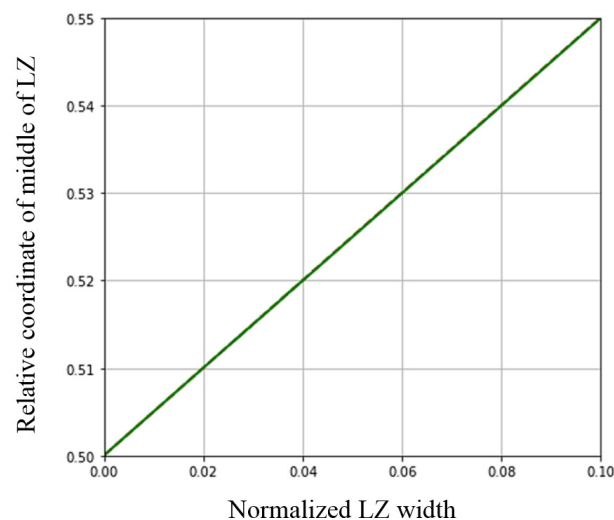
**Figure 8.** Results of the reconstruction of the light zone width by the video signal  $v(\hat{t})$  (solid line—for the conventional method for the reconstruction using the first derivative of the video signal  $v(\hat{t})$ ; dashed line—for the reconstruction with the use of the SSPs): (a) the dependence of the measured values of the normalized width of the LZ on the real values of the width; (b) relative error of the LZ width determination depending on its real value.

Figure 9 presents the results of the measurements of the normalized light zone brightness. For normalization, the zone brightness value was taken as 1. Brightness was computed with the use of the SSPs in accordance with expression (27). When the LZ brightness was reconstructed by the conventional method, the extremum of the observed multiscan video signal  $v(\hat{t})$  was found. The analysis of the diagrams in Figure 9a shows that in the region of narrow zones, the conventional method gives a significant loss of brightness. It is associated with the smearing of the LZ rectangular pulse by the multiscan and the “depression” of the pulse amplitude, especially in the region of a narrow zone, which is illustrated in Figure 2. Conversely, the determination of the light zone brightness by the offered method using the SSPs allows for a highly accurate reconstruction of its value in the region of narrow zones as well. Figure 9b shows the dependencies of the relative error in the LZ brightness determination. From the analysis of the dependencies, it follows that the use of the conventional method for the reconstruction of the amplitude of the smeared narrow rectangular pulse is impossible due to the high error values. In the case of the use of the SSPs, there is the possibility of the highly-accurate reconstruction of the LZ brightness for very narrow zones.



**Figure 9.** Results of the reconstruction of the light zone brightness by the video signal  $v(\hat{t})$  (solid line—the conventional method for the reconstruction by the signal  $v(\hat{t})$ ; dashed line—the reconstruction with the use of SSPs): (a) the dependence of the measured values of the normalized brightness of the light zone on the real values of its normalized width; (b) relative error of the LZ brightness determination depending on the real value of its normalized width.

Figure 10 presents the results of the experiments on the localization of the light spot on the multiscan surface for LZs of different widths. For this, in the centre of the multiscan, a light zone was formed. The left edge of the zone remained immobile and its coordinate corresponded to the value of 0.5. The right edge of the zone was moved to the right, making the zone wider (as it had been in the previous experiments). In this case, the middle of the LZ also moved to the right. For each state of the light zone, the coordinate of the middle of the LZ was determined by the observed signal  $v(\hat{t})$  with the use of the two methods: first, by the traditional method as the arithmetic average of the extrema coordinates of the first derivative of the video signal  $v(\hat{t})$ , and then by the offered method with the use of the SSPs in accordance with expression (28). Both diagrams in Figure 10 coincide, which indicates the same accuracy of the light spot localization on the multiscan by both methods over the entire range of the LZ width values.



**Figure 10.** The results of the determination of the coordinates of the middle of the light zone by a video signal  $v(\hat{t})$ .

#### 4. Conclusions

The modelling results show that when the television multiscan operates in the analogue mode at the LZ width exceeding the volt aperture  $VA \geq 8U_0$ , the video signal is of a trapezoidal shape, and at the decrease of the zone width to the moment of its disappearance—of a bell shape.

It is shown that for small objects (corresponding to narrow light zones), the moments of the change of the sign of the second derivative of the video signal do not correspond to the boundaries of this zone due to the smearing-out of the video signal by its volt aperture, which does not provide a high accuracy of the measurements of the geometric parameters of these objects.

The mechanism is considered to be the video signal formation based on the multiscan impulse response, which is defined as an elementary video signal from an infinitely narrow light zone—from one discrete photodiode cell of the multiscan.

It is established that the convolution of the signal of the rectangular profile of a light zone with the impulse response explains the smearing-out of the video signal edges; in this case, the smearing-out value is fully determined by the impulse response and does not depend on the zone width.

A method is offered for the full reconstruction of the rectangular profile of a light zone (including a narrow one) in the developed noise-proof optoelectronic measuring device based on a multiscan with the use of spatio-structural parameters, where the light zone profile width corresponds to the extent of illumination—brightness, and its coordinate—centroid.

It is shown that the subtraction of the impulse response dissipation from the video signal dissipation permits taking into account the value of the video signal smearing-out with high accuracy at the estimation of the light zone width, in correspondence with the property of the additive accumulation of dissipation.

It is established that the use of the spatio-structural model of a video signal allows for widening the sphere of application of the multiscan-based optoelectronic devices for the tasks of highly-accurate control and measurement of the geometric parameters of small objects. However, the issues of increasing the accuracy of measurements of structural elements' dimensions in noisy graphic images using SSPs have not been sufficiently investigated.

In the future, we can use other techniques such as holographic interferometry [32,33], or machine vision system with MATLAB [32], Edge Directions [34], and using logic models and sensors [35].

**Author Contributions:** Conceptualization, M.Y.A., Y.K.S. and A.I.K.; methodology, M.Y.A., A.A.M. and I.O.A.; formal analysis, M.Y.A. and A.I.K.; writing—original draft preparation, Y.K.S., I.O.A. and A.A.M.; writing—review and editing, V.T. and I.K.; supervision, I.K., M.S. and M.Y.A.; funding acquisition, V.T. and M.S. All authors have read and agreed to the published version of the manuscript.

**Funding:** This article was funded by the University of Žilina project 313011ASY4 - "Strategic implementation of additive technologies to strengthen the intervention capacities of emergencies caused by the COVID-19 pandemic".

**Institutional Review Board Statement:** Not applicable.

**Informed Consent Statement:** Not applicable.

**Data Availability Statement:** The data presented in this study are available on request from the corresponding author.

**Conflicts of Interest:** The authors declare no conflict of interest.

## References

1. Božek, P.; Lozkin, A.; Gorbushin, A. Geometrical Method for Increasing Precision of Machine Building Parts. In Proceedings of the International Conference on Manufacturing Engineering and Materials, ICMEM 2016, Nový Smokovec, Slovakia, 6–10 June 2016; Volume 149, pp. 576–580. [\[CrossRef\]](#)
2. Vopat, T.; Peterka, J.; Kovac, M.; Buransky, I. The Wear Measurement Process of Ball Nose End Mill in the Copy Milling Operations. In Proceedings of the 24th DAAAM International Symposium on Intelligent Manufacturing and Automation, 2013, Zadar, Croatia, 23–26 October 2013; Volume 69, pp. 1038–1047. [\[CrossRef\]](#)
3. Buranský, I.; Morovič, L.; Peterka, J. Application of Reverse Engineering for Redesigning and Manufacturing of a Printer Spare Part. *Adv. Mater. Res.* **2013**, *690–693*, 2708–2712. [\[CrossRef\]](#)
4. Abbasi, A.R.; Mahmoudi, M.R. Application of Statistical Control Charts to Discriminate Transformer Winding Defects. *Electr. Power Syst. Res.* **2021**, *191*, 106890. [\[CrossRef\]](#)
5. Alies, M.Y.; Shelkovnikov, Y.K.; Sága, M.; Vaško, M.; Kuric, I.; Shelkovnikov, E.Y.; Korshunov, A.I.; Meteleva, A.A. Method and Device Based on Multiscan for Measuring the Geometric Parameters of Objects. *Processes* **2020**, *9*, 24. [\[CrossRef\]](#)
6. Saha, O.; Dasgupta, P. Experience Learning From Basic Patterns for Efficient Robot Navigation in Indoor Environments. *J. Intell. Robot. Syst.* **2018**, *92*, 545–564. [\[CrossRef\]](#)
7. Sahawneh, L.R.; Wikle, J.K.; Roberts, A.K.; Spencer, J.C.; McLain, T.W.; Warnick, K.F.; Beard, R.W. Ground-Based Sense-and-Avoid System for Small Unmanned Aircraft. *J. Aerosp. Inf. Syst.* **2018**, *15*, 501–517. [\[CrossRef\]](#)
8. Guk, E.; Podlaskin, B. Novel Principle of Optical Signal Sensing Based on the Creation of Signal Statistical Estimates. In Proceedings of the IEEE Sensors, Limerick, Ireland, 28–31 October 2011; pp. 436–439. [\[CrossRef\]](#)
9. Podlaskin, B.; Guk, E.; Sukharev, A. Registration Technique for Detection of Optical Signal Position under Intense Background Illumination. In Proceedings of the 2014 3rd Mediterranean Conference on Embedded Computing (MECO), Budva, Montenegro, 15–19 June 2014; IEEE: Piscataway, NJ, USA; pp. 232–235. [\[CrossRef\]](#)
10. Podlaskin, B.; Guk, E. New Optical Sensor with Continuous Field of View for Real-Time Signal Processing. In Proceedings of the 2012 Mediterranean Conference on Embedded Computing (MECO), Bar, Montenegro, 19–21 June 2012; pp. 104–107.
11. Lipanov, A.M.; Shelkovnikov, Y.K. The Use of a Television Scanistor in Dual Use Devices. *Izv. RARAN* **2005**, *2*, 71. (In Russian)
12. Shelkovnikov, Y.K.; Lipanov, A.M. *Theoretical Basics and Manufacturing Technology of Television Scanistor Structures*; Ural Branch of the Russian Academy of Sciences: Yekaterinburg, Russia, 2005.
13. Lipanov, A.M.; Shelkovnikov, Y.K. Manufacturing Technology of Epitaxial Scanistor Sensors. *Izv. RARAN* **2005**, *43*, 75–79. (In Russian)
14. Horton, J.W.; Mazza, R.V.; Dym, H. The Scanistor—A Solid-State Image Scanner. *Proc. IEEE* **1964**, *52*, 1513–1528. [\[CrossRef\]](#)
15. Podlaskin, B.G.; Guk, E.G. The Multiscan Position-Sensitive Photodetector. *Meas. Tech.* **2005**, *48*, 779–783. [\[CrossRef\]](#)
16. Mahmoudi, M.R.; Nematollahi, A.R.; Soltani, A.R. On the Detection and Estimation of the Simple Harmonizable Processes. *Iran. J. Sci. Technology. Trans. A Sci.* **2015**, *39*, 239–242.
17. Lipanov, A.M.; Shelkovnikov, Y.K.; Osipov, N.I. Application of Discrete-Continuous Multi-Scan Structure in Optoelectronic Measuring Devices. *Sensors Syst.* **2003**, *2*, 46–49. (In Russian)
18. Podlaskin, B.G.; Guk, E.G.; Obolenskov, A.G.; Sukharev, A.A. Suppression of the Effect of High-Power Background Illumination on the Precision of Determination of the Optical Signal Coordinates. *Tech. Phys.* **2015**, *60*, 1384–1387. [\[CrossRef\]](#)
19. Lipanov, A.M.; Shelkovnikov, Y.K.; Osipov, N.I. The Analysis of Multiscan Operation with Amplitude-Modulated Optical Signals. *Sensors Syst.* **2003**, *10*, 12–16. (In Russian)
20. Shelkovnikov, Y.K. Improving the Stability and Linearity of a Coordinate Characteristic of Scanistor Information and Measuring Systems. *Intell. Syst. Prod.* **2011**, *17*, 251–255. (In Russian)
21. Podlaskin, B.G. Spatial Filtering of Temporal Noise with the Hadamard Transformation Applied to a Photodetector Array. *Tech. Phys.* **2007**, *52*, 672–675. [\[CrossRef\]](#)
22. Podlaskin, B.G.; Guk, E.G.; Nosenko, E.V. Multiscan-Based Double Synthetic Aperture for Locating the Illuminance Boundary of a Weak Optical Signal. *Tech. Phys.* **2002**, *47*, 726–730. [\[CrossRef\]](#)
23. Shelkovnikov, Y.K.; Osipov, N.I.; Kiznertsev, S.R.; Meteleva, A.A. Influence of the Photoresistive Effect of Multiscan Resistive Dividers on Accuracy of Measurements of Geometrical Parameters of Objects. *Intell. Syst. Manuf.* **2018**, *16*, 57–64. [\[CrossRef\]](#)
24. Shelkovnikov, Y.K.; Osipov, N.I.; Kiznertsev, S.R.; Meteleva, A.A. Analysis of Influence of Kinetics of the TV Multicast Photocurrent on the Error of Measuring the Coordinates and Sizes of Light Zones. *Vestn. IzhGTU Im. M.T. Kalashnikova* **2019**, *22*, 89–99. [\[CrossRef\]](#)
25. Podlaskin, B.G.; Guk, E.G. Analog Processor Based on the Multiscan Photoreceiver for the Aperture Correction of the Median of a Dis-Torted Optical Signal. *Zhurnal tekhnicheskoy Fiz.* **2006**, *76*, 93–98. (In Russian)
26. Abbasi, A.R.; Mahmoudi, M.R.; Arefi, M.M. Transformer Winding Faults Detection Based on Time Series Analysis. *IEEE Trans. Instrum. Meas.* **2021**, *70*, 3516210. [\[CrossRef\]](#)
27. Bailey, D.; Wright, E. *Practical Fiber Optics*; Newnes: London, UK, 2003; ISBN 9780080473871.
28. Koltsov, P.P. Estimation of Image Blurring. *Comput. Opt.* **2011**, *35*, 95–102. (In Russian)
29. Murynov, A.I. Estimation of the Geometric and Topological Parameters of Image Details Based on the Method of Centroid Filtration. *Chem. Phys. Mesoscopy* **2002**, *4*, 161–177. (In Russian)

30. Arkhipov, I.O. Modeling and Analysis of Linear Low-Sized Structural Elements of Graphics Images on the Basis of Usage of Spatially Chromatic Parameters. *Vestn. IzhGTU Im. M.T. Kalashnikova* **2014**, *2*, 149–152. (In Russian)
31. Arkhipov, I.O.; Shelkovnikov, Y.K.; Meteleva, A.A. The Use of the Spatial-Structural Model of a Video Signal from the Television Scanistor in Tasks of Monitoring the Geometric Parameters of Small Objects. In Proceedings of the Journal of Physics: Conference Series, Samara, Russia, 26–29 May 2020; Volume 1745, pp. 638–644. [[CrossRef](#)]
32. Černecký, J.; Božek, P.; Pivarčiová, E. A New System For Measuring The Deflection Of The Beam With The Support Of Digital Holographic Interferometry. *J. Electr. Eng.* **2015**, *66*, 53–56. [[CrossRef](#)]
33. Božek, P.; Pivarčiová, E. Registration of Holographic Images Based on Integral Transformation. *Comput. Inform.* **2012**, *31*, 1369–1383.
34. Karrach, L.; Pivarčiová, E.; Božek, P. Identification of QR Code Perspective Distortion Based on Edge Directions and Edge Projections Analysis. *J. Imaging* **2020**, *6*, 67. [[CrossRef](#)]
35. Nikitin, Y.; Božek, P.; Peterka, J. Logical–Linguistic Model of Diagnostics of Electric Drives with Sensors Support. *Sensors* **2020**, *20*, 4429. [[CrossRef](#)]

**Disclaimer/Publisher’s Note:** The statements, opinions and data contained in all publications are solely those of the individual author(s) and contributor(s) and not of MDPI and/or the editor(s). MDPI and/or the editor(s) disclaim responsibility for any injury to people or property resulting from any ideas, methods, instructions or products referred to in the content.